

Empagliflozin improves chronic hypercortisolism-induced abnormal myocardial structure and cardiac function in mice

Qing-Qing Zhang, Guo-Qing Li, Yi Zhong, Jie Wang, An-Ning Wang, Xiao Zhou and Xiao-Ming Mao

Abstract

Background: Chronic exposure to excess glucocorticoids is frequently associated with a specific cardiomyopathy. Empagliflozin, a sodium-glucose cotransporter 2 (SGLT2) inhibitor, has beneficial effects as it aids in the reduction of heart failure and cardiovascular mortality in hospitalized patients. The aim of this study was to investigate the effects of empagliflozin on chronic hypercortisolism-induced myocardial fibrosis and myocardial dysfunction in mice.

Methods: Male C57BL/6J mice (6 weeks old) were randomized to control, corticosterone (CORT), and empagliflozin + CORT groups. After 4 weeks of administration, heart structure and function were evaluated by echocardiography, and peripheral blood and tissue samples were collected. Expressions of *Ccl2*, *Itgax*, *Mrc1*, and *Adgre1* mRNA in heart tissue were evaluated by RT-PCR, and signal transducer and activator of transcription 3 (STAT3) and Toll-like receptor 4 (TLR4) protein expression were analyzed by Western blotting.

Results: Empagliflozin effectively reduced body weight, liver triglyceride, visceral adipose volume, and uric acid in CORT-treated mice. Left ventricular hypertrophy and cardiac dysfunction were improved significantly, phosphorylated STAT3 and TLR4 were alleviated, and macrophage infiltration in the myocardium was inhibited after administration of empagliflozin in CORT-treated mice.

Conclusion: Empagliflozin has beneficial effects on specific cardiomyopathy associated with CORT, and the results provide new evidence that empagliflozin might be a potential drug for the prevention of this disease.

Keywords: hypercortisolism, myocardial hypertrophy, myocardial fibrosis, SGLT2 inhibitor

Received: 6 August 2020; revised manuscript accepted: 29 October 2020.

Introduction

Chronic exposure to excess glucocorticoids (GCs) may result from either endogenous exposure, like in Cushing's Syndrome (CS), or exogenous exposure, like in patients who received GC treatment.^{1,2} CS is a severe disease due to complications induced by excess GCs. Excess GCs can cause hypertension,³ metabolic changes, coagulopathy, and specific complications of the heart and vasculature.^{4,5} The incidence of cardiovascular morbidity and mortality in patients with CS is usually high. As revealed by echocardiography, about 70% of

patients with active CS have showed abnormal left ventricular (LV) mass parameters. Increased myocardial fibrosis has been found in 42% and concentric remodeling in 23% of these patients.⁶ Another study has also suggested that increased myocardial fibrosis is present in CS patients compared with healthy controls and hypertensive patients, as assessed by echocardiography.⁷ Changes in autonomic cardiac regulation may contribute to cardiovascular risk. Electrocardiograph (ECG) findings have revealed changes in the QT interval, which is considered to be a CS-specific feature due to the

Ther Adv Chronic Dis

2020, Vol. 11: 1–12

DOI: 10.1177/
2040622320974833

© The Author(s), 2020.
Article reuse guidelines:
[sagepub.com/journals-](https://sagepub.com/journals-permissions)
permissions

Correspondence to:

Xiao-Ming Mao
Department of
Endocrinology, Nanjing
First Hospital, Nanjing
Medical University, 68
ChangLe St., Nanjing,
210006, China
maoxming@163.com

Qing-Qing Zhang
Department of
Endocrinology, Nanjing
First Hospital, Nanjing
Medical University,
Nanjing, China

Department of
Endocrinology, Taizhou
People's Hospital, Jiangsu,
China

Guo-Qing Li
Yi Zhong
Jie Wang
An-Ning Wang
Xiao Zhou
Department of
Endocrinology, Nanjing
First Hospital, Nanjing
Medical University,
Nanjing, China

cardiotoxic effect of the cortisol excess despite the presence of other risk factors.⁸ Reduced heart rate (HR) variability has also been observed in CS patients.^{9,10} It is worth noting that the cardiometabolic syndrome still progresses in some patients despite achieving long-term remission after medical treatment.¹¹ Currently, there is no ideal treatment strategy for preventing tissue-specific consequences of hypercortisolism.

Empagliflozin, a sodium-glucose cotransporter 2 (SGLT2) inhibitor, is an oral hypoglycemic agent that reduces hyperglycemia by blocking renal glucose reabsorption in the renal proximal tubules in an insulin-independent manner.¹² Empagliflozin is a potent inhibitor of SGLT2 that does not increase the risk of bone fractures and amputations.^{13–15} In addition to its role in maintaining good glycemic control, empagliflozin also reduces blood pressure and body weight significantly in diabetic patients. Furthermore, it has been found that empagliflozin can alleviate heart failure and cardiovascular mortality in high-risk individuals with type 2 diabetes mellitus (T2DM).^{16–18} In prediabetic mice, empagliflozin can improve coronary microvascular function and cardiac contractility.¹⁹ SGLT2 inhibitors also exhibit beneficial cardioprotection effects in non-diabetic patients with heart failure.^{17,20}

However, the effects of SGLT2 inhibitors on cardiovascular diseases induced by chronic excessive intake of GC are not fully understood. The present study thus aimed to assess the efficacy of empagliflozin in preventing chronic hypercortisolism-induced specific cardiomyopathy, including inflammation, myocardial fibrosis, and echocardiographic features.

Materials and methods

Animals and experimental protocol

All methods were carried out in accordance with the guidelines and regulations of Nanjing Medical University (China), and all animal procedures were authorized and specifically approved by the institutional ethical committee of Nanjing Hospital Affiliated to Nanjing Medical University (No. 1905292).

All mice were purchased from the Comparative Medicine Centre of Yangzhou University (China). Male C57BL/6J mice (6 weeks old; weight 16–22 g)

were housed in cages (4–6 per cage) with *ad libitum* access to water and normal chow. Mice were kept in a temperature-, humidity-, and light-controlled environment (12-h light/dark cycle). Subsequently, animals were randomized into groups (15 per group) and raised for 4 weeks. The groups were as follows: (1) vehicle group (VEH): oral receiving tap water with a final ethanol concentration of 0.66%; (2) CORT group: oral receiving tap water containing corticosterone (100 µg/ml) dissolved in ethanol (0.66%); (3) CORT + empagliflozin (CORT + EM) group: oral receiving tap water containing corticosterone (CORT:100 µg/ml) and empagliflozin (10 mg/kg/day, the dosage of empagliflozin in every mouse was 0.16–0.22 mg/day, oral gavage, 0.5% hydroxyethyl cellulose was used as the vehicle). Empagliflozin was provided by Dalian Meilun Biotechnology Co., LTD (Dalian, China).

Echocardiographic evaluation

Transthoracic echocardiography was performed using non-invasive Doppler ultrasound at the end of the study period in all mice using a high-frequency ultrasound imaging system (Vevo 2100 VisualSonics, Inc., Toronto, Ontario, Canada). As previously described,²¹ HR and the following structural variables were evaluated: LV end-diastolic diameter (LVEDD), LV end-systolic diameter (LVESD), interventricular septal thickness in systole (IVSs) and in diastole (IVSd), and LV posterior wall thickness in systole (LVPWs) and diastole (LVPWd). LV function was assessed by the following parameters including fractional shortening (FS), ejection fraction (EF), and E/A ratio. The mean values of six consecutive cardiac cycles were obtained for all indicators. All measurements were conducted by a single investigator who was blinded to the experimental groups.

Calculated heart liver and epididymal fat weight index

At the end of the study period, the mice in each group were weighed and measured tibia length after pentobarbital (1.5%) anesthesia. The heart, liver, and epididymal white adipose tissue (eWAT) were removed, washed with precooled phosphate-buffered saline, dried with filter paper, and weighed. The heart weight to tibia length ratio (mg/mm), liver weight to body weight ratio (mg/g), and eWAT weight to body weight ratio (mg/g) were calculated.

Table 1. Primers for qPCR.

Gene name	Forward primer	Reverse primer
<i>Ccl2</i>	TCCACTACCTTTTCCACAACCA	CGCACAGAGTGGATGTCGTC
<i>Itgax</i>	CAGAGCCAGAACTTCCCAACT	ATCTGTGGAAGTATGCTACCC
<i>Mrc1</i>	GACGAAAGGCGGGATGTGT	TGGGTTTCAGGAGTTGTTGTGG
<i>Adgre1</i>	TCCTACACTATCTTTTCTCGCC	CCTTCAGGTTTCTCACCATCAG
qPCR, quantitative real-time PCR.		

Biochemical analyses

Fasting blood was obtained from the orbital venous plexus in heparin-coated tubes. Blood was centrifuged to separate plasma from whole blood and stored at -80°C until analysis. The levels of serum insulin and CORT were tested by enzyme-linked immunosorbent assay (ELISA) kit (Wuhan Cloud-Clone Biotechnology Co., LTD, Wuhan, China). Plasma total cholesterol (TC), triglyceride (TG), low-density lipoprotein cholesterol (LDL-C), high-density lipoprotein cholesterol (HDL-C), glucose (FPG), alanine aminotransferase (ALT), aspartate aminotransferase (AST), and uric acid (UA) were determined by chemiluminescence. The homeostasis model assessment of insulin resistance (HOMA-IR) was calculated using the following formula: $\text{FPG (mmol/l)} \times \text{fasting plasma insulin (mIU/l)} \div 22.5$.

Liver TG content

After a 6-h fast, all TGs in mouse liver tissues were extracted and analyzed using TG assay kits (Nanjing Jiancheng Biotechnology Co., LTD, Nanjing, China), according to the manufacturer's instructions.

Histological and immunohistochemical analysis

Heart tissues were fixed in 4% paraformaldehyde, dehydrated, paraffin-embedded, sectioned at $4\ \mu\text{m}$ thickness, and mounted on glass slides. The anterolateral sections from hearts were evaluated the extent of fibrosis in cardiac muscle (Masson's trichrome staining) and cardiomyocyte cross-sectional area in myocardial sections [*wheat germ agglutinin* (WGA) staining]. Connective tissue is stained blue, nuclei are stained dark purple, and cytoplasm is stained red after Masson's trichrome staining. Paraffin-embedded heart sections were stained immunohistochemically for F4/80 and transforming growth factor- $\beta 1$ (TGF- $\beta 1$) as

previously described.²² The quantification of the positive area was calculated by ImageJ software (version 1.50; <https://imagej.nih.gov/ij/>).

RNA extraction and quantitative real-time PCR

Total RNA was extracted from myocardium using TRIzol reagent (Thermo Fisher Scientific, Waltham, MA, USA) and reverse-transcribed into complementary DNA (cDNA) with a PrimeScript Reverse Transcription Master Mix (TaKaRa, Shiga, Japan), according to the protocol per manufacturer's instruction. Quantitative real-time PCR (qPCR) was performed with TB Green premix Ex Taq II (TaKaRa) on an Applied Biosystems 7500 Real-Time PCR System (Applied Biosystems, Foster City, CA, USA). In order to analyze relative gene expression with real-time PCR, we selected two reference genes: β -actin and glyceraldehyde 3-phosphate dehydrogenase (GAPDH). The intra- and inter-assay variation was tested. The real-time PCR efficiency of the two reference genes was similar, and expression of the two reference genes was constant. We selected GAPDH as reference gene and expression of the target gene was normalized to GAPDH. The primers listed in Table 1. Relative expression levels were calculated using the cycle threshold ($2^{-\Delta\Delta\text{Ct}}$) method.

Western blotting analysis

Toll-like receptor 4 (TLR4) (Affinity Biosciences Cat# AF7017, RRID: AB_2835322; Affinity Biosciences, Cincinnati, OH, USA), total signal transducer and activator of transcription 3 (T-STAT3) (Affinity Biosciences Cat# AF6294, RRID: AB_2835144) and its phosphorylated (Affinity Biosciences Cat# AF3293, RRID: AB_2810278) form in heart muscle were evaluated by Western blotting. Samples were homogenized in a lysis buffer, sonicated, and centrifuged.

Protein concentration was determined using a bicinchoninic acid (BCA) protein quantitation assay. Protein (40 µg) were separated by 10% SDS-PAGE, transferred to polyvinylidene difluoride (PVDF) membranes, blocked with 5% bovine serum albumin (BSA) [in *Tris-buffered* saline with 0.1% Tween 20 (TBST)] for 2 h at room temperature and then incubated with primary antibodies overnight at 4°C. The membranes were then washed and incubated with secondary horseradish peroxidase-conjugated antibodies for 1 h at room temperature. After washing with TBST, bands were detected using the enhanced chemifluorescence reagent. The intra- and inter-assay variation was tested in GAPDH and β-actin, and western blotting efficiency of the two reference proteins were similar and constant. Band intensity was quantified by scanning densitometry using Image J software and normalized to GAPDH (Affinity Biosciences Cat# AF7021, RRID: AB_2839421).

Statistical analysis

Results are presented as mean ± standard deviation (SD). Differences between the mean values were determined using one-way ANOVAs with Tukey's *post hoc* correction (GraphPad Prism; GraphPad, San Diego, CA, USA), with $p < 0.05$ as significant.

Results

Effect of empagliflozin on weight gain and serum parameters

The weight gain and serum parameters of the mice in the three groups are summarized in Table 2. Body weight, heart weight, heart weight/tibial length, liver weight, liver weight/body weight, and liver TG content in CORT-treated mice were significantly higher than those in the VEH and CORT + EM groups ($p < 0.05$ or 0.001). However, there were no statistically significant differences in these indexes between the VEH and CORT + EM groups ($p > 0.05$). The eWAT weight and eWAT weight/body weight in the CORT + EM group significantly was lower after 4 weeks of prevention compared with that in the CORT group ($p < 0.05$ or 0.001), but these indices were still higher than those in the VEH group. The level of plasma CORT was significantly higher in the CORT and CORT + EM groups compared with the VEH group ($p < 0.05$). Meanwhile, the levels of insulin

and HOMA-IR were significantly higher in the CORT and CORT + EM groups compared with the VEH group ($p < 0.05$), and there were no significant differences in the levels of insulin and HOMA-IR between the CORT and CORT + EM groups ($p > 0.05$). The levels of TC, HDL-C, LDL-C, and TG also were significantly higher in the CORT and CORT + EM groups compared with the VEH group ($p < 0.05$); however, there were no significant differences in these indices between the CORT + EM group and CORT group ($p > 0.05$). The UA level was significantly higher in the CORT group than in the VEH and CORT + EM groups ($p < 0.05$). There were no statistical differences in the levels of fasting blood glucose, ALT, and AST in the three groups at the end of the study period.

Effect of empagliflozin on LV dimensions and functions in CORT-treated mice

As shown in Figure 1 and Table 3, the HR of mice in the CORT + EM group was significantly lower after 4 weeks of administration of empagliflozin compared with that of mice in the CORT group, but it was still higher than that in the VEH group. There was obvious impairment in LV mass, LV mass/body weight ratio, IVSd, IVSs, and LVPWd in the CORT group. Administration of empagliflozin could largely restore LV mass, LV mass/body weight ratio, IVSd, IVSs, and LVPWd in CORT-treated mice, which were similar to those in the VEH group. There were no significant differences in the values of LVEDD, LVESD, and IVSs among the three groups. CORT administration lead to lower EF and FS, which was significantly improved by empagliflozin. Furthermore, empagliflozin could simultaneously inhibit the reduction of diastolic function (E/A).

Empagliflozin inhibits myocardial hypertrophy and myocardial fibrosis in CORT-treated mice

Histological sections were stained with fluorescein isothiocyanate-labeled WGA to determine cell size. The mean cardiomyocyte size in the CORT group was significantly larger than that in the VEH group ($p < 0.05$, Figure 2A, B), and the CORT + EM group exhibited a significantly smaller cardiomyocyte size ($p < 0.05$).

Masson's trichrome staining was performed to evaluate the degree of cardiac fibrosis. As shown

Table 2. Weight gain and serum parameters.

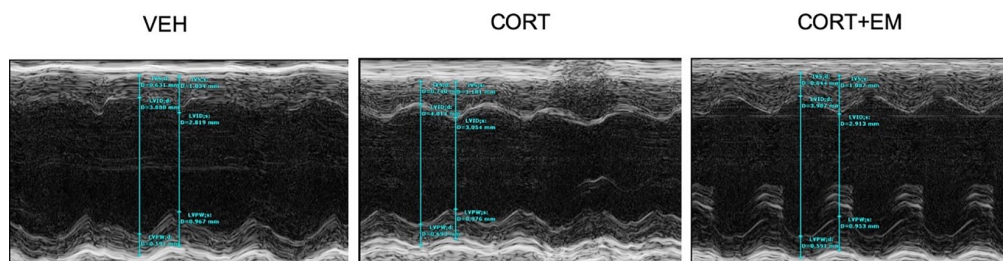
	VEH (n=15)	CORT (n=15)	CORT + EM (n=15)	p value
Body weight (g)	23.63 ± 0.87	24.74 ± 0.69*	23.01 ± 0.71#	<0.001
Heart weight (mg)	133.43 ± 6.11	139.45 ± 6.82*	132.13 ± 6.75#	0.008
Heart weight/tibial length (mg/mm)	7.41 ± 0.35	7.75 ± 0.28*	7.34 ± 0.37#	0.004
Liver weight (mg)	912.5 ± 79.86	1087.50 ± 137.08*	905.00 ± 61.23#	<0.001
Liver weight/body weight (mg/g)	38.63 ± 2.64	43.95 ± 5.94*	39.69 ± 4.01#	0.005
Liver TG content (mmol/g protein)	3.43 ± 0.73	6.45 ± 1.11*	4.20 ± 0.93#	<0.001
eWAT weight (mg)	197.50 ± 5.00	745.00 ± 115.61*	265.00 ± 26.46**	<0.001
eWAT weight/body weight (mg/g)	8.36 ± 0.15	30.10 ± 4.54*	11.62 ± 1.10**	<0.001
Fasting blood glucose (mmol/l)	5.53 ± 0.43	5.72 ± 1.11	5.25 ± 0.66	0.268
Insulin (ng/ml)	0.74 ± 0.08	14.38 ± 2.17*	13.71 ± 3.01*	<0.001
HOMA-IR	4.49 ± 0.35	82.55 ± 17.60*	79.09 ± 9.95*	<0.001
TC (mmol/l)	77.83 ± 3.17	201.17 ± 12.87*	202.54 ± 11.93*	<0.001
TG (mmol/l)	91.40 ± 7.82	289.10 ± 25.66*	273.49 ± 25.08*	<0.001
HDL-C (mmol/l)	59.71 ± 3.11	75.27 ± 5.38*	73.93 ± 4.51*	<0.001
LDL-C (mmol/l)	12.08 ± 1.08	60.26 ± 5.22*	61.69 ± 5.14*	<0.001
ALT (U/l)	67.94 ± 16.92	72.89 ± 10.20	59.37 ± 21.05	0.092
AST (U/l)	120.51 ± 17.66	124.87 ± 17.79	118.13 ± 10.47	0.496
UA (mmol/l)	109.78 ± 25.12	144.56 ± 29.49*	112.01 ± 28.46#	0.002
CORT (ng/ml)	47.32 ± 8.40	201.73 ± 93.28*	196.08 ± 84.17*	<0.001

Data are expressed as the mean ± SD.

ALT, alanine aminotransferase; AST, aspartate aminotransferase; CORT, corticosterone; EM, empagliflozin; eWAT, epididymal white adipose tissue; HDL-C, high-density lipoprotein cholesterol; HOMA-IR, homeostasis model assessment of insulin resistance; LDL-C, low-density lipoprotein cholesterol; SD, standard deviation; TC, total cholesterol; TG, triglyceride; UA, uric acid; VEH, vehicle group.

**p* < 0.05 versus VEH.

#*p* < 0.05 versus CORT.

**Figure 1.** LV echocardiographic representative images.

CORT, corticosterone group; CORT+EM, CORT + empagliflozin group; LV, left ventricular; VEH, vehicle group.

Table 3. Echocardiographic assessment of left ventricle structural and functional data in mice.

	VEH (n = 10)	CORT (n = 10)	CORT + EM (n = 10)	p value
Heart rate (bpm)	438.67 ± 30.71	497.92 ± 17.78*	460.22 ± 21.35#	<0.001
LVEDD (mm)	3.83 ± 0.28	3.94 ± 0.24	4.00 ± 0.32	0.405
LVESD (mm)	2.81 ± 0.27	3.01 ± 0.21	2.93 ± 0.22	0.179
IVSd (mm)	0.63 ± 0.06	0.76 ± 0.03*	0.66 ± 0.05#	<0.001
IVSs (mm)	1.05 ± 0.08	1.17 ± 0.05*	1.08 ± 0.05#	<0.001
LVPWd (mm)	0.60 ± 0.03	0.71 ± 0.06*	0.63 ± 0.04#	<0.001
LVPWs (mm)	0.99 ± 0.05	0.98 ± 0.04	0.98 ± 0.04	0.840
LV mass (mg)	74.82 ± 11.94	101.78 ± 9.02*	88.03 ± 13.11#	<0.001
LV mass/body weight (mg/g)	3.14 ± 0.13	4.11 ± 0.15*	3.83 ± 0.10**	<0.001
EF (%)	56.58 ± 2.86	45.61 ± 1.55*	53.86 ± 2.23#	<0.001
FS (%)	29.09 ± 1.68	22.50 ± 0.79*	26.73 ± 1.15**	<0.001
E/A	1.57 ± 0.09	1.25 ± 0.11*	1.47 ± 0.10#	<0.001

Data are presented as the mean ± SD.
 CORT, corticosterone; E/A, ratio between early (E)-to-late (A) diastolic mitral inflow; EF, ejection fraction; EM, empagliflozin; FS, fractional shortening; IVSd, interventricular septal width during end-diastole; IVSs: systolic interventricular septal thickness; LV, left ventricle; LVEDD, Left ventricular end-diastolic diameter; LVESD, Left ventricular end-systolic diameter; SD, standard deviation; VEH, vehicle group.
 **p* < 0.05 versus VEH.
 #*p* < 0.05 versus CORT.

in Figure 2A and C, there was significantly more collagen deposition in the CORT group compared with the VEH group (*p* < 0.05). The administration of empagliflozin alleviated CORT-induced collagen deposition markedly, as shown by the downregulation of the fibrosis ratio (*p* < 0.05). Furthermore, the anti-fibrosis effects of empagliflozin were also verified by the reduction in the expression of pro-fibrotic proteins TGF-β1 compared with the CORT group, as seen through immunohistochemical staining of TGF-β1 (*p* < 0.05, Figure 2A, D).

Empagliflozin attenuates CORT-induced infiltration of macrophage in mouse heart

Based on the results of the immunostaining and mRNA expression of F4/80, empagliflozin was found to lower markedly the infiltration of macrophage in the mouse myocardium (*p* < 0.05, Figure 3A, B). M1 macrophages (*Itgax*) and

MCP-1 (*Ccl2*) levels were significantly higher in CORT-treated mice than in the VEH and CORT + EM groups (*p* < 0.05, Figure 3B), whereas the mRNA level of M2 macrophages (*Mrc1*) was significantly lower in CORT-treated mice than in the CORT + EM group (*p* < 0.05, Figure 3B).

Effect of empagliflozin on TLR-4 and Stat3 pathway in mouse heart

Western blot analysis of TLR-4 protein expression levels showed that TLR-4 level in the CORT + EM group was lower dramatically compared with the CORT group (*p* < 0.05, Figure 4A).

Western blot analysis showed that phosphorylation of STAT3 at Tyr705 was activated by CORT (*p* < 0.05), and empagliflozin inhibited significantly the phosphorylation of STAT3 (*p* < 0.05, Figure 4B).

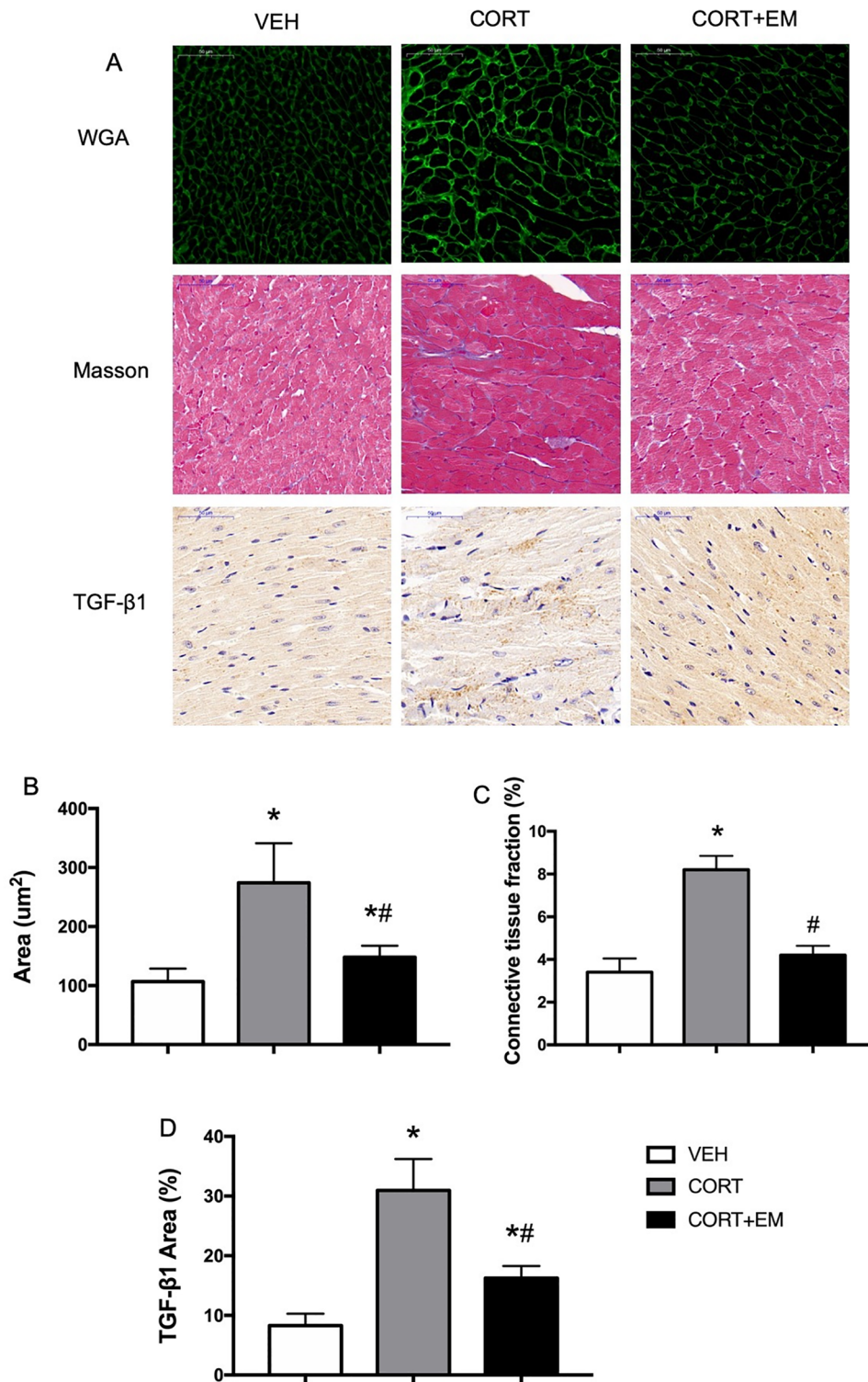


Figure 2. Empagliflozin suppresses myocardial hypertrophy and fibrosis in CORT-treated mice. WGA staining, immunostaining of TGF-β1 protein expression, and Masson's trichrome staining of the myocardium (A). Cardiomyocyte cross-sectional area (B), connective tissue fraction (C), and the percentages of positive areas of TGF-β1 (D). Data are expressed as mean ± SD.

* $p < 0.05$ versus VEH.

$p < 0.05$ versus CORT.

CORT, corticosterone group; CORT+EM, CORT + empagliflozin group; SD, standard deviation; TGF-β1, transforming growth factor-β 1; VEH, vehicle group; WGA, wheat germ agglutinin.

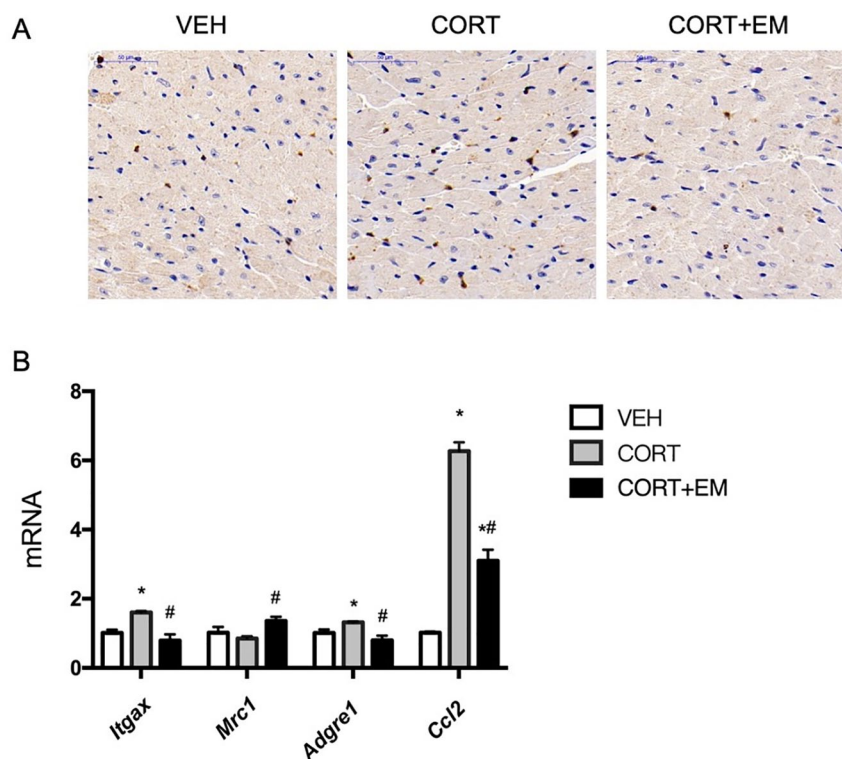


Figure 3. Macrophage infiltration in myocardium. Immunofluorescence images of macrophage antibody F4/80 (A). mRNA expression of macrophage markers (*Adgre1*, *Mrc1*, *Itgax*, and *Ccl2*) (B). Values are expressed as means \pm SD.

* $p < 0.05$ versus VEH.

$p < 0.05$ versus CORT.

CORT, corticosterone group; CORT+EM, CORT + empagliflozin group; SD, standard deviation; VEH, vehicle group.

Discussion

The key findings of this study were that administration of empagliflozin significantly ameliorated systolic and diastolic LV function, cardiac hypertrophy, and fibrosis, and inhibited the infiltration of macrophages, especially M1 macrophages, in the myocardial tissue in CORT-treated mice. Furthermore, empagliflozin could effectively reduce body weight, liver TG, visceral adipose tissue, and UA, but it may not improve insulin resistance.

Impairment of cardiac function, such as LV hypertrophy, concentric remodeling, and diastolic and systolic dysfunction, has been reported in CS patients using echocardiography.^{6,23} Consistent with previous studies, although CORT did not affect LV diameters in our study, LV hypertrophy and impairment of LV diastolic and systolic function were obvious in the CORT-treated mice compared with the VEH group. The WGA staining of myocardial tissue suggested that severe myocardial fibrosis was found in the CORT

group, and that the size of myocardial cells was larger than those in the VEH group. These structural and pathological abnormalities might be attributed to GC excess, which leads to increased blood pressure by the stimulation of both mineralocorticoid and GC receptors and activation of the components of the renin-angiotensin system that enhances angiotensin-II responsiveness of the myocytes.^{24,25} More importantly, GC excess can induce the development of myocardial fibrosis directly, thus contributing significantly to the development of cardiac dysfunction, independent of LV hypertrophy.⁷

In the present study, administration of empagliflozin for 4 weeks successfully improved the cardiac structural and functional abnormalities in CORT-treated mice. It has been reported that cardiac function was improved in a female rodent model of diabetes and in a non-diabetic pressure overload-induced heart failure mouse model by empagliflozin.^{26,27} Consistent with our study, empagliflozin significantly attenuated cardiac fibrosis in both

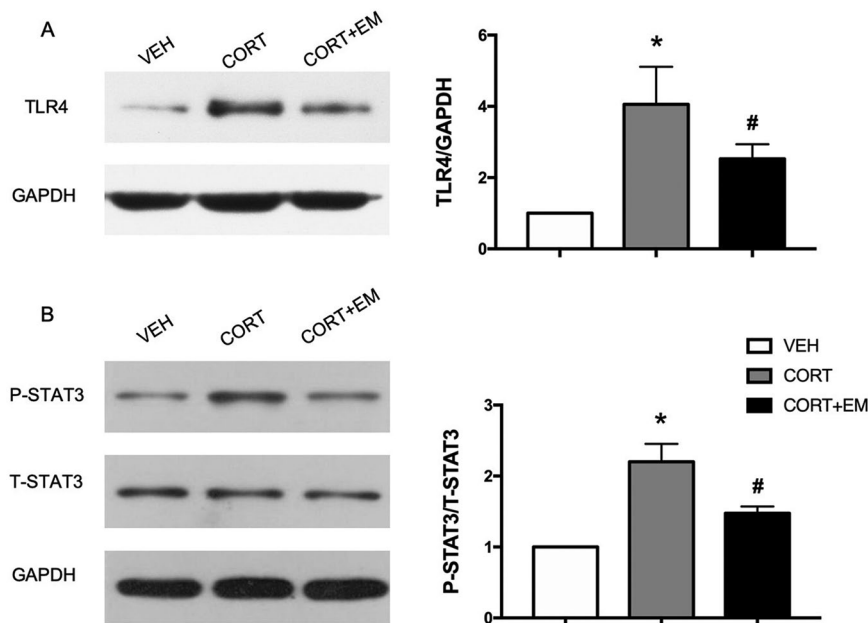


Figure 4. Representative immunoblots and quantitative analysis of TLR4 (A), STAT3 (B). Values are expressed as means \pm SD.

* $p < 0.05$ versus VEH.

$p < 0.05$ versus CORT.

CORT, corticosterone group; CORT+EM, CORT + empagliflozin group; STAT3, Signal transducer and activator of transcription 3; T-STAT3, total STAT3; P-STAT3, phosphorylated STAT3; GAPDH, glyceraldehyde 3-phosphate dehydrogenase; SD, standard deviation; TLR4, Toll-like receptor 4; VEH, vehicle group.

atrial and ventricular tissues of rats with hypertensive heart failure.²⁸ In addition to the heart, empagliflozin also exerts an anti-fibrotic effect on models of experimental diabetes nephropathy.²⁹ Therefore, the beneficial effects of SGLT2 inhibitors on attenuation of fibrosis and improvement of structural and functional abnormalities might be independent of its glucose-lowering effects.

Macrophage phenotypes have been shown to influence myocardial remodeling. Here, we found that macrophages, especially M1 macrophages was greatly increased in the myocardial tissue of CORT-treated mice. Meanwhile, we also found that empagliflozin can significantly downregulate the level of F4/80 and promote M1 toward M2 macrophage phenotype transition in the myocardial tissue of CORT-treated mice. STAT3 signaling has also been shown to be involved in macrophage polarization,³⁰ and angiotensin-II-mediated cardiac remodeling depends on phosphorylation of STAT3 through TLR4.³¹ TLR4 knockout significantly attenuated angiotensin-II-induced STAT3 activation, resulting in preservation of cardiac dysfunction

and myocardial remodeling.³¹ Moreover, Matsuda *et al.* demonstrated that TLR4 deficiency reversed angiotensin-II-induced cardiac hypertrophy, macrophage infiltration, and diastolic dysfunction.³² In the present study, we found that CORT could activate STAT3 and upregulate the expression of TLR4 in mouse myocardium. While empagliflozin could downregulate the expression of TLR4 and the ratio of p-STAT3/STAT3. Therefore, empagliflozin may alleviate CS-associated cardiomyopathy by inhibiting the phosphorylation of STAT3, downregulating the expression of TLR4, and inhibiting macrophage infiltration in the myocardium. We must acknowledge that the diabetes-independent cardiovascular protective effects of empagliflozin may also benefit from its diuretic effect,³³ improvement of energy metabolism, and establishing a powerful synergy with the metabolic substrate shift in myocardial cells.^{34–36} The exact mechanisms of the pleiotropic effects of empagliflozin on improving heart performance in the specific cardiomyopathy associated with GC use requires further experiments and research for it to be fully elucidated.

In this study, we also evaluated the influence of empagliflozin on the metabolic comorbidities that may affect the cardiac function in CORT-treated mice. A previous study suggested that empagliflozin can reduce the plasma glucose concentration threshold to <40 mg/dl, which is well below the normal fasting plasma glucose concentration in individuals without diabetes.³⁷ However, we did not find an effect of empagliflozin on plasma glucose levels in CORT-treated mice. This might be due to interference of CORT or the difference between humans and mice, and the exact reason needs to be studied further. The decline in the UA level with empagliflozin may be due to the increased UA excretion due to glycosuria. The present findings also indicated beneficial effects of empagliflozin on the reduction of body weight, the weight of eWAT, and improvement of fatty livers in CORT-treated mice. Although many studies have found that SGLT2 inhibitors could improve insulin resistance and reduce serum lipid levels, some studies have put forward different views. Dapagliflozin, another SGLT2 inhibitor, had no effect on tissue-level insulin sensitivity, as seen through PET/CT imaging findings in obese patients with type 2 diabetes.³⁸ There were no changes in LDL-C or TG levels in DM patients after treatment with empagliflozin.³⁹ Therefore, the mechanism of effect of SGLT2 inhibitors on blood lipids and insulin resistance needs further exploration.

We must acknowledge that there are some limitations to our study. First, the data on the effects of empagliflozin on blood pressure, energy metabolism, myocardial oxidative stress, intramyocardial sodium and calcium regulation, and HR variability were not available. Second, the animals were not housed in individual cages, making the urine collection a bulk collection. This bulk urine sample was analyzed for information such as urine volume, glucosuria, albuminuria, urinary CORT, and electrolyte excretion.

Conclusion

Empagliflozin exerted beneficial effects on UA, liver TGs, and visceral adipose tissue in mice exposed to CORT. It also ameliorated myocardial fibrosis, hypertrophy, and dysfunction in the same group. The potential application of the SGLT2 inhibitor empagliflozin in conditions beyond T2DM may include CS-associated cardiomyopathy.

Conflict of interest statement

The authors declare that there is no conflict of interest.

Funding

The authors disclosed receipt of the following financial support for the research, authorship, and/or publication of this article: This work was supported by National Natural Science Foundation of China (81570710).

References

1. Arnaldi G, Angeli A, Atkinson AB, *et al.* Diagnosis and complications of Cushing's syndrome: a consensus statement. *J Clin Endocrinol Metab* 2003; 88: 5593–5602.
2. Overman RA, Yeh JY and Deal CL. Prevalence of oral glucocorticoid usage in the United States: a general population perspective. *Arthritis Care Res (Hoboken)* 2013; 65: 294–298.
3. Fielders RA, Pulgar SJ, Kempel A, *et al.* The burden of Cushing's disease: clinical and health-related quality of life aspects. *Eur J Endocrinol* 2012; 167: 311–326.
4. Rizzoni D, Porteri E, De Ciuceis C, *et al.* Hypertrophic remodeling of subcutaneous small resistance arteries in patients with Cushing's syndrome. *J Clin Endocrinol Metab* 2009; 94: 5010–5018.
5. Duprez DA. Role of the renin-angiotensin-aldosterone system in vascular remodeling and inflammation: a clinical review. *J Hypertens* 2006; 24: 983–991.
6. Baykan M, Erem C, Gedikli O, *et al.* Assessment of left ventricular diastolic function and Tei index by tissue Doppler imaging in patients with Cushing's syndrome. *Echocardiography* 2008; 25: 182–190.
7. Yiu KH, Marsan NA, Delgado V, *et al.* Increased myocardial fibrosis and left ventricular dysfunction in Cushing's syndrome. *Eur J Endocrinol* 2012; 166: 27–34.
8. Alexandraki KI, Kaltsas GA, Vouliotis AI, *et al.* Specific electrocardiographic features associated with Cushing's disease. *Clin Endocrinol (Oxf)* 2011; 74: 558–564.
9. Fallo F, Maffei P, Dalla Pozza A, *et al.* Cardiovascular autonomic function in Cushing's syndrome. *J Endocrinol Invest* 2009; 32: 41–45.
10. Chandran DS, Ali N, Jaryal AK, *et al.* Decreased autonomic modulation of heart rate and altered cardiac sympathovagal balance in patients with Cushing's syndrome: role of endogenous

- hypercortisolism. *Neuroendocrinology* 2013; 97: 309–317.
11. Aranda G, Fernandez-Ruiz R, Palomo M, *et al.* Translational evidence of prothrombotic and inflammatory endothelial damage in Cushing syndrome after remission. *Clin Endocrinol (Oxf)* 2018; 88: 415–424.
 12. De Leeuw AE and De Boer RA. A translational viewpoint explaining its potential salutary effects. *Eur Heart J Cardiovasc Pharmacother* 2016; 2: 257.
 13. Yurista SR, Sillje HHW, Van Goor H, *et al.* Effects of sodium-glucose co-transporter 2 inhibition with empagliflozin on renal structure and function in non-diabetic rats with left ventricular dysfunction after myocardial infarction. *Cardiovasc Drugs Ther* 2020; 34: 311–321.
 14. Matthews DR, Li Q, Perkovic V, *et al.* Effects of canagliflozin on amputation risk in type 2 diabetes: the CANVAS Program. *Diabetologia* 2019; 62: 926–938.
 15. Inzucchi SE, Iliev H, Pfarr E, *et al.* Empagliflozin and assessment of lower-limb amputations in the EMPA-REG OUTCOME trial. *Diabetes Care* 2018; 41: e4–e5.
 16. Damman K, Beusekamp JC, Boorsma EM, *et al.* Randomized, double-blind, placebo-controlled, multicentre pilot study on the effects of empagliflozin on clinical outcomes in patients with acute decompensated heart failure (EMPA-RESPONSE-AHF). *Eur J Heart Fail* 2020; 22: 713–722.
 17. Packer M, Anker SD, Butler J, *et al.* Cardiovascular and renal outcomes with empagliflozin in heart failure. *N Engl J Med* 2020; 383: 1413–1424.
 18. Zinman B, Wanner C, Lachin JM, *et al.* Empagliflozin, cardiovascular outcomes, and mortality in type 2 diabetes. *N Engl J Med* 2015; 373: 2117–2128.
 19. Adingupu DD, Göpel SO, Grönros J, *et al.* SGLT2 inhibition with empagliflozin improves coronary microvascular function and cardiac contractility in prediabetic ob/ob(-/-) mice. *Cardiovasc Diabetol* 2019; 18: 16.
 20. McMurray JJV, Solomon SD, Inzucchi SE, *et al.* Dapagliflozin in patients with heart failure and reduced ejection fraction. *N Engl J Med* 2019; 381: 1995–2008.
 21. Rosa CM, Gimenes R, Campos DHS, *et al.* Apocynin influence on oxidative stress and cardiac remodeling of spontaneously hypertensive rats with diabetes mellitus. *Cardiovasc Diabetol* 2016; 15: 126.
 22. Li C, Zhang J, Xue M, *et al.* SGLT2 inhibition with empagliflozin attenuates myocardial oxidative stress and fibrosis in diabetic mice heart. *Cardiovasc Diabetol* 2019; 18: 15.
 23. Pereira AM, Delgado V, Romijn JA, *et al.* Cardiac dysfunction is reversed upon successful treatment of Cushing's syndrome. *Eur J Endocrinol* 2010; 162: 331–340.
 24. Singh Y, Kotwal N and Menon AS. Endocrine hypertension - Cushing's syndrome. *Indian J Endocrinol Metab* 2011; 15(Suppl. 4): S313.
 25. Sharma ST and Nieman LK. Cushing's syndrome: all variants, detection, and treatment. *Endocrinol Metab Clin North Am* 2011; 40: 379–391, viii–ix.
 26. Habibi J, Aroor AR, Sowers JR, *et al.* Sodium glucose transporter 2 (SGLT2) inhibition with empagliflozin improves cardiac diastolic function in a female rodent model of diabetes. *Cardiovasc Diabetol* 2017; 16: 9.
 27. Byrne NJ, Parajuli N, Levasseur JL, *et al.* Empagliflozin prevents worsening of cardiac function in an experimental model of pressure overload-induced heart failure. *JACC Basic Transl Sci* 2017; 2: 347–354.
 28. Lee HC, Shiou YL, Jhuo SJ, *et al.* The sodium-glucose co-transporter 2 inhibitor empagliflozin attenuates cardiac fibrosis and improves ventricular hemodynamics in hypertensive heart failure rats. *Cardiovasc Diabetol* 2019; 18: 45.
 29. Ojima A, Matsui T, Nishino Y, *et al.* Empagliflozin, an inhibitor of sodium-glucose cotransporter 2 exerts anti-inflammatory and antifibrotic effects on experimental diabetic nephropathy partly by suppressing AGEs-receptor axis. *Horm Metab Res* 2015; 47: 686–692.
 30. Lee TM, Chang NC and Lin SZ. Dapagliflozin, a selective SGLT2 inhibitor, attenuated cardiac fibrosis by regulating the macrophage polarization via STAT3 signaling in infarcted rat hearts. *Free Radic Biol Med* 2017; 104: 298–310.
 31. Han J, Ye S, Zou C, *et al.* Angiotensin II causes biphasic STAT3 activation through TLR4 to initiate cardiac remodeling. *Hypertension* 2018; 72: 1301–1311.
 32. Matsuda S, Umemoto S, Yoshimura K, *et al.* Angiotensin activates MCP-1 and induces cardiac hypertrophy and dysfunction via toll-like receptor 4. *J Atheroscler Thromb* 2015; 22: 833–844.
 33. McMurray J. EMPA-REG - the “diuretic hypothesis”. *J Diabetes Complications* 2016; 30: 3–4.

34. Ferrannini E, Mark M and Mayoux E. CV protection in the EMPA-REG OUTCOME trial: a “thrifty substrate” hypothesis. *Diabetes Care* 2016; 39: 1108–1114.
35. Yurista SR, Sillje HHW, Oberdorf-Maass SU, *et al.* Sodium-glucose co-transporter 2 inhibition with empagliflozin improves cardiac function in non-diabetic rats with left ventricular dysfunction after myocardial infarction. *Eur J Heart Fail* 2019; 21: 862–873.
36. Mudaliar S, Alloju S and Henry RR. Can a shift in fuel energetics explain the beneficial cardiorenal outcomes in the EMPA-REG OUTCOME study? A unifying hypothesis. *Diabetes Care* 2016; 39: 1115–1122.
37. Al-Jobori H, Daniele G, Cersosimo E, *et al.* Empagliflozin and kinetics of renal glucose transport in healthy individuals and individuals with type 2 diabetes. *Diabetes* 2017; 66: 1999–2006.
38. Latva-Rasku A, Honka MJ, Kullberg J, *et al.* The SGLT2 inhibitor dapagliflozin reduces liver fat but does not affect tissue insulin sensitivity: a randomized, double-blind, placebo-controlled study with 8-week treatment in type 2 diabetes patients. *Diabetes Care* 2019; 42: 931–937.
39. Kohler S, Salsali A, Hantel S, *et al.* Safety and tolerability of empagliflozin in patients with type 2 diabetes. *Clin Ther* 2016; 38: 1299–1313.

Visit SAGE journals online
[journals.sagepub.com/
home/taj](http://journals.sagepub.com/home/taj)

 SAGE journals